Vol. 353: 81–88, 2008
doi: 10.3354/meps07151

MARINE ECOLOGY PROGRESS SERIES
Mar Ecol Prog Ser

Published January 17

In situ observation of phytoplankton productivity by an underwater profiling buoy system: use of fast repetition rate fluorometry

Tetsuichi Fujiki[1,2,5,*], Takuji Hosaka[1,2], Hideshi Kimoto[3], Takashi Ishimaru[4], Toshiro Saino[1,2]

[1]Hydrospheric Atmospheric Research Center, Nagoya University, Chikusa-ku, Nagoya 464-8601, Japan
[2]Japan Science and Technology Agency, Kawaguchi Center Building, 4-1-8, Honcho, Kawaguchi, Saitama 332-0012, Japan
[3]Kimoto Electric Co., Ltd., 3-1 Funahashi-cho, Tennoji-ku, Osaka 543-0024, Japan
[4]Faculty of Marine Science, Tokyo University of Marine Science and Technology, 4-5-7, Konan, Minato-ku, Tokyo 108-8477, Japan

[5]*Present address:* Mutsu Institute for Oceanography, Japan Agency for Marine-Earth Science and Technology, 690 Kitasekine, Sekine, Mutsu, Aomori 035-0022, Japan

ABSTRACT: To gain a better understanding of variability in phytoplankton productivity in the oceans, we developed an underwater profiling buoy system that uses a fast repetition rate (FRR) fluorometer. We used the profiling buoy system to observe phytoplankton productivity in Sagami Bay, Japan, from 15 April to 10 May 2005. During the observation period, chlorophyll *a* (chl *a*) concentration increased gradually, peaking at >5 mg chl *a* m^{-3} at a depth of 10 m, indicating the occurrence of phytoplankton blooms. Gross oxygen production (P_{O2}), as determined by FRR fluorometry, increased with the development of phytoplankton blooms and peaked at 49.4 mmol O_2 m^{-2} h^{-1} on 2 May 2005, when both the chl *a* concentration and surface irradiance were high. To validate FRR-based P_{O2}, the light-utilization efficiency of a water column (ψ_{O2}) was calculated and compared with previous values determined for this location by the oxygen evolution method. The ψ_{O2} derived from FRR fluorometry showed good agreement with those by the oxygen evolution method, suggesting that FRR fluorometry was able to roughly estimate *in situ* daily P_{O2}. Our profiling buoy system has potential benefits for the measurement of oceanic phytoplankton productivity at a high resolution.

KEY WORDS: FRR fluorometry · Gross oxygen production · Phytoplankton blooms · Profiling buoy system

INTRODUCTION

An understanding of the variability in phytoplankton productivity provides a basic knowledge of the structure and functioning of aquatic ecosystems. The primary productivity of the world oceans has been measured mainly by the radiocarbon tracer (Steemann Nielsen 1952) or the oxygen evolution (Williams et al. 1983) methods. As these traditional methods use the uptake of radiocarbon into particulate matter or changes in oxygen concentration in the bulk fluid, measurements require bottle incubations for periods ranging from hours to 1 day. This methodological limitation has hindered our understanding of the variability of oceanic primary productivity. To overcome these problems, algorithms for estimating primary productivity by using satellite ocean color imagery have been developed and improved (Behrenfeld et al. 2002 and references cited therein). However, one of the major obstacles to this is a lack of *in situ* primary productivity data to verify the satellite estimates.

*Email: tfujiki@jamstec.go.jp

During the past decade, the utilization of active fluorescence techniques in biological oceanography has brought marked progress to our understanding of phytoplankton photosynthesis in the oceans (Falkowski & Kolber 1995). Above all, fast repetition rate (FRR) fluorometry reduces the primary electron acceptor (Q_a) in photosystem II (PSII) by a series of subsaturating flashlets and can measure a single turnover fluorescence induction curve in PSII (Kolber et al. 1998). The PSII parameters derived from the fluorescence induction curve provide information on the physiological state related to photosynthesis and can be used to estimate gross primary productivity. The utility of FRR fluorometry in measuring *in situ* productivity has been examined by several groups (Suggett et al. 2001, Moore et al. 2003, Raateoja et al. 2004, Smyth et al. 2004, Corno et al. 2005, Sarma et al. 2006). Although the uncertainty of several assumptions (e.g. photosynthetic unit size of PSII [n_{PSII}], ratio of PSII electron transport for O_2 evolution [$1/k$], and the ratio of evolved O_2 to fixed CO_2 [R]) could introduce errors, these studies have suggested that FRR fluorometry is a promising method for estimating gross primary productivity. FRR fluorometry has several advantages over the above-mentioned traditional methods. Most importantly, because measurements made by FRR fluorometry can be carried out without the need for time-consuming bottle incubations, this method enables real-time high-frequency measurements of primary productivity. In addition, the FRR fluorometer can be used in platform systems such as moorings, drifters, and floats.

We developed an underwater profiling buoy system that uses the FRR fluorometer and observed the vertical and temporal variations in PSII parameters and primary productivity in Sagami Bay, Japan, over about a month. The detailed observations made by the profiling buoy system successfully provided information on the variability of *in situ* productivity. To the best of our knowledge, this is the first attempt at using a profiling buoy system to observe changes in oceanic primary productivity.

MATERIALS AND METHODS

Custom-built FRR fluorometer. To measure fluorescence induction curves *in situ*, we constructed a submersible FRR fluorometer (Diving Flash, Kimoto Electric) (Fig. 1). The Diving Flash consists of closed dark and open light chambers that measure the fluorescence induction curves on dark-adapted and ambient-irradiated samples. The embedded central processing unit (CPU) (SH7727, Hitachi) supervised the operation of the Diving Flash. For each optical channel in the dark and light chambers, the Diving Flash has a high-luminosity blue light-emitting diode (LED) (LXHL-LB5C, Philips Lumileds Lighting) that excites chlorophyll *a* (chl *a*) fluorescence at a wavelength of 470 nm with a 25 nm bandwidth. Excitation light was focused on the target by using a plano-convex lens. To cumulatively saturate PSII within 150 µs (Kolber et al. 1998), this instrument generated a sequence of flashes at a repetition rate of about 250 kHz s^{-1} and provided an excitation light intensity of 30 mmol quanta m^{-2} s^{-1} by adjusting a pulsed current to the LED. The intensity of the excitation light emitted by the LED was measured with a radiometer (LI-190SA, Li-Cor) with a fast amplifier. The fluorescence signal from phytoplankton exposed to the excitation light was collected at a 90° angle, isolated by a band-pass filter at a wavelength of 685 nm with a 25 nm bandwidth (F25-685, CVI Laser), and detected by a photomultiplier tube (PMT) (R1925A, Hamamatsu Photonics KK). Simultaneously, a small portion of the excitation light was recorded by a PIN photodiode (S5971, Hamamatsu Photonics KK) as a reference signal. Both the fluorescence and refer-

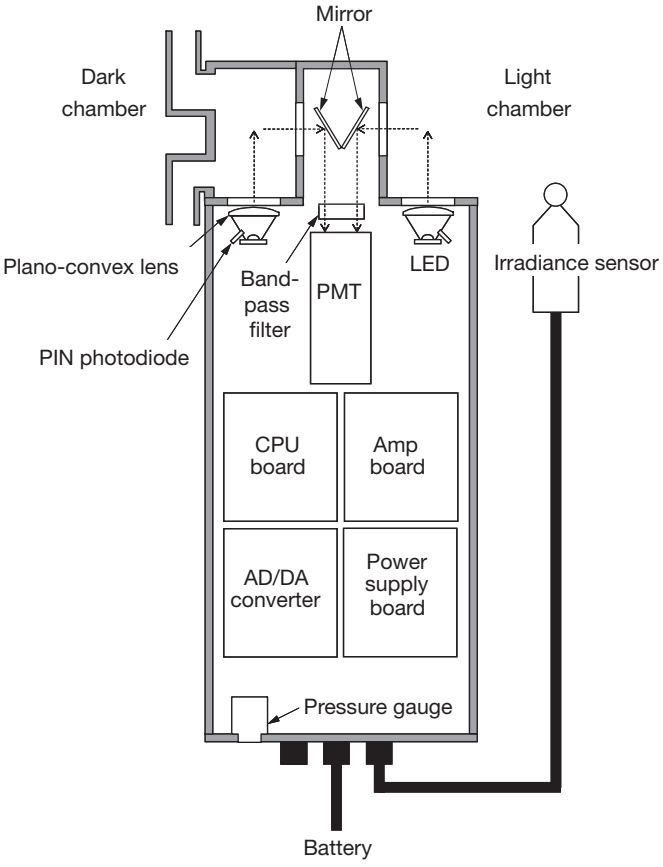

Fig. 1. Schematic block diagram of the custom-built FRR fluorometer (Diving Flash, Kimoto Electric)

ence signals were synchronously converted at 10 MHz by a 14-bit analog-to-digital converter (AD9240, Analog Devices) and analyzed by a CPU.

The fluorescence induction curve measured with the Diving Flash is presented in Fig. 2. The fluorescence yield was calculated as the ratio of the fluorescence signal to the reference signal. Baseline, scatter, and reference functions were corrected by the method of Laney (2003). The model was fitted to the fluorescence induction curves by using custom-written software in accordance with the procedure described by Kolber et al. (1998). Analysis of fluorescence induction curves measured in the dark and light chambers provided PSII parameters such as F_0, F_m, F', F_m', σ_{PSII}, σ_{PSII}' (see Table 1 for parameter definitions; all parameters measured in the light chamber are identified by the prime symbol). A single excitation sequence consisted of 50 subsaturation flashlets, each 2 µs long, at 4 µs intervals. Each acquisition in the dark and light chambers consisted of 25 single excitation sequences, and measurements in the dark and light chambers were made alternately in sequence. Irradiance (E) and depth were simultaneously measured by a scalar irradiance sensor (QSP-2200, Biospherical Instruments) and a pressure gauge (ABH500PSC1B, Honeywell International), respectively, incorporated within the instrument (Fig. 1).

Table 1. Definitions of PSII parameters

Parameter	Definition
$\int \mathrm{chl}a(z)\mathrm{d}z$	Integrated chl *a* concentration from the surface to the base of the euphotic layer (mg chl *a* m^{-2})
E	Irradiance (µmol quanta m^{-2} s^{-1})
E_0	Surface irradiance (µmol quanta m^{-2} s^{-1})
$\int E_0(t)\mathrm{d}t$	E_0 integrated over a day (mol quanta m^{-2} d^{-1})
F_0	Minimum fluorescence yield in darkness (dimensionless)
F_m	Maximum fluorescence yield in darkness (dimensionless)
F_v/F_m	Potential photochemical efficiency of open reaction centers [= $(F_m - F_0)/F_m$; dimensionless]
F_0'	Minimum fluorescence yield under actinic light {= $F_0/[(F_v/F_m)+(F_0/F_m')]$; dimensionless}
F'	Fluorescence yield at any point between F_0' and Fm′ (dimensionless)
F_m'	Maximum fluorescence yield under actinic light (dimensionless)
F_q'/F_v'	PSII efficiency factor under actinic light [= $(F_m' - F')/(F_m' - F_0')$; dimensionless]
n_{PSII}	Photosynthetic unit size of PSII (0.002 mol RCII mol chl a^{-1})
P_{O2}	Gross oxygen production (mmol O_2 m^{-3} h^{-1})
$\int P_{O2}(z)\mathrm{d}z$	Integrated P_{O2} from the surface to the base of the euphotic layer (mmol O_2 m^{-2} h^{-1})
$\iint P_{O2}(t, z)\mathrm{d}z\mathrm{d}t$	Integrated P_{O2} from the surface to the base of the euphotic layer over 1 day (mmol O_2 m^{-2} d^{-1})
R	Ratio of evolved O_2 to fixed CO_2 (mol O_2 mol C^{-1})
$1/k$	Ratio of PSII electron transport for O_2 evolution (0.25 mol O_2 mol electron^{-1})
σ_{PSII}	Effective absorption cross section of PSII in darkness (Å^2 quanta^{-1})
σ_{PSII}'	Effective absorption cross section of PSII under actinic light (Å^2 quanta^{-1})
ψ_{O2}	Light utilization efficiency of a water column (mmol O_2 m^2 mg chl a^{-1} mol quanta^{-1})

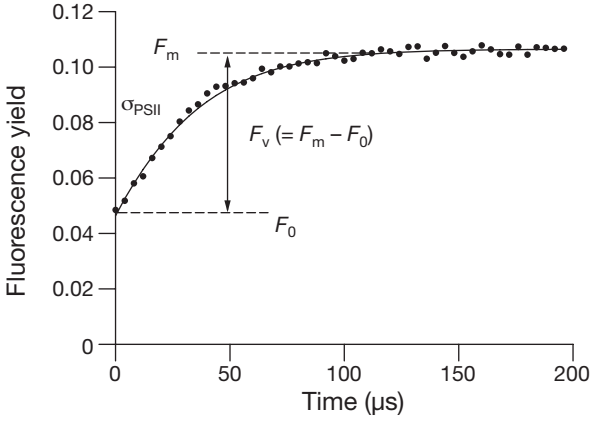

Fig. 2. Example of fluorescence induction curve measured with the Diving Flash on alga *Dunaliella tertiolecta* (Chlorophyceae). A series of 50 subsaturating flashlets, each 2 µs long, was used to cumulatively saturate PSII within 150 µs. PSII parameters F_0, F_m, σ_{PSII} were derived by numerically fitting the fluorescence induction curve to the model in accordance with the procedure described by Kolber et al. (1998)

In accordance with the method of Suggett et al. (2006), gross oxygen production (P_{O2}, mmol O_2 m^{-3} h^{-1}) can be determined by substituting the PSII parameters measured into the following equation:

$$P_{O2} = E\,\sigma_{PSII}'\,n_{PSII}\,(1/k)\,(F_q'/F_v')\,[\mathrm{chl}\,a] \times 0.0243 \quad (1)$$

where F_q'/F_v' is the PSII efficiency factor under actinic light ($[F_m' - F']/[F_m' - F_0']$), [chl *a*] is the chl *a* concentration (mg chl *a* m^{-3}) estimated by the F_m value, and the factor 0.0243 converts seconds to hours, µmol quanta to mol quanta, Å^2 to m^2, and mol chl *a* to mg chl *a*. Minimum fluorescence yield under actinic light (F_0') was estimated from $F_0/[(F_v/F_m) + (F_0/F_m')]$ (Oxborough & Baker 1997). Chl *a* concentrations were computed from F_m after a significant linear regression was obtained between F_m and chl *a* concentration in discrete seawater samples (Fig. 3).

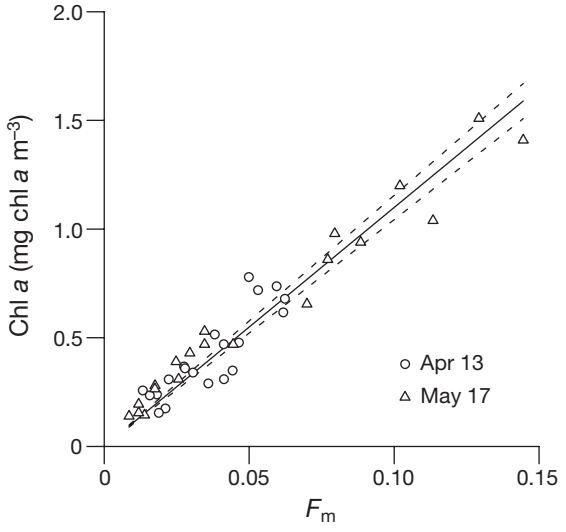

Fig. 3. Relationship between maximum fluorescence yield in darkness (F_m) and chl *a* concentration in discrete seawater samples ($r^2 = 0.92$, n = 40, $p < 0.05$, slope = 11.0). The discrete samples were obtained from 0 to 100 m in the forenoon on 13 April (before mooring) and 17 May 2005 (after mooring). (– – –): 95% CI

Underwater profiling buoy system. The underwater profiling buoy system consisted mainly of an observation buoy equipped with the Diving Flash, a CTD sensor, an underwater winch, and an acoustic releaser (Nichiyu Giken Kogyo; Fig. 4). The observation buoy moved between the winch depth (150 m) and the surface at a rate of 0.2 m s^{-1} and measured the vertical profiles of phytoplankton fluorescence, irradiance, temperature, and salinity. The profiling rate of the observation buoy was set to 0.2 m s^{-1} to detect small-scale variations (approx. 0.5 m) in the vertical profile. In addition, the profiling rate at 0.2 m s^{-1} allowed samples in the dark chamber to dark-adapt for about 1 s before measurements. Once the observation buoy reached the surface, it transmitted the measured data to the shore-based laboratory by mobile phone and returned to the winch depth. To minimize biofouling of instruments, the underwater winch was placed below the euphotic layer so that the observation buoy was exposed to light only during the measurement period. The vertical migration of the observation buoy also reduced biofouling. During the observation period, the F_m values at about 150 m (pseudo-blanks) were low

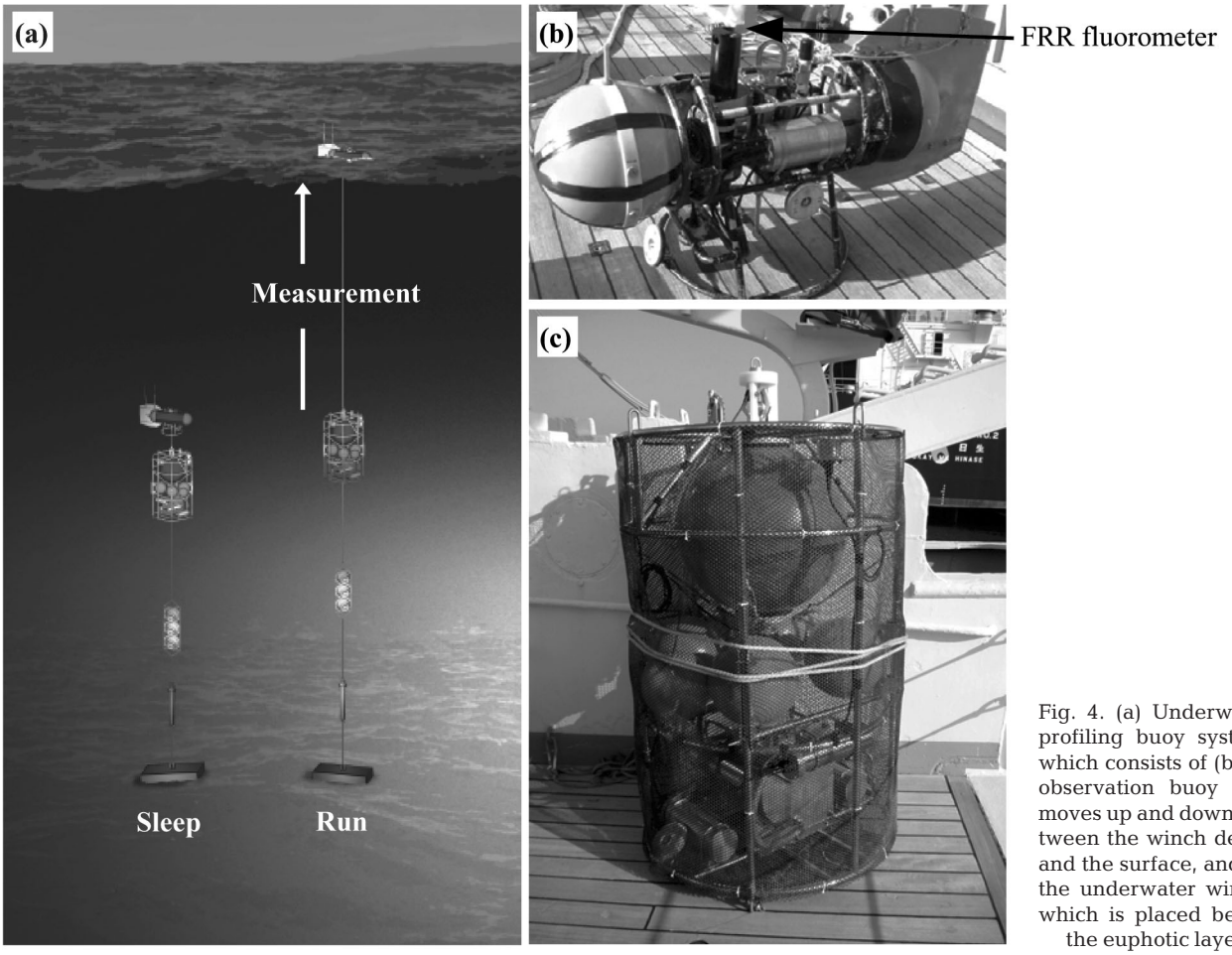

Fig. 4. (a) Underwater profiling buoy system, which consists of (b) an observation buoy that moves up and down between the winch depth and the surface, and (c) the underwater winch, which is placed below the euphotic layer

and constant (0.004 ± 0.001), suggesting that the influence of biofouling was very little.

In the near-surface layers, ambient red light interferes with FRR measurements (red light effect) (Raateoja et al. 2004). In the coastal waters of the Baltic Sea, Raateoja et al. (2004) observed that the water layer affected by the red light effect was the upper 2 to 3 m. In addition, as the Diving Flash shares a single photomultiplier with the dark and light chambers (Fig. 1), the red light effect not only restricts the light chamber measurements but also influences the dark chamber measurements. Hence, for the present study, the data in the surface layer (upper ~3 m) was removed.

Site description and observations. The profiling buoy system was placed at Stn S3 in Sagami Bay (35° 00′ N, 139° 20′ E, depth ~1500 m) (Fig. 5). The system was moored by R/V 'Seiyo Maru' of the Tokyo University of Marine Science and Technology. Sagami Bay is strongly influenced by the Kuroshio Current, which runs along the eastern coast of Japan. Oligotrophic oceanic waters mix with eutrophic riverine waters in the bay, and rich blooms of diatoms or dinoflagellates are often observed from April to June (Nakata 1985, Fujiki et al. 2004). Measurements with the profiling buoy system were made at 10:00 h daily from 15 April to 10 May 2005. In addition, measurements for estimating the daily P_{O2} were taken at 2 h intervals from 8:00 h (after sunrise) to 18:00 h (before sunset) on 18 and 25 April and 9 May 2005.

To validate the daily P_{O2} derived from the FRR fluorometry data, the light-utilization efficiency of a water column (ψ_{O2}) was calculated from integrated P_{O2} from the surface to the base of the euphotic layer over 24 h

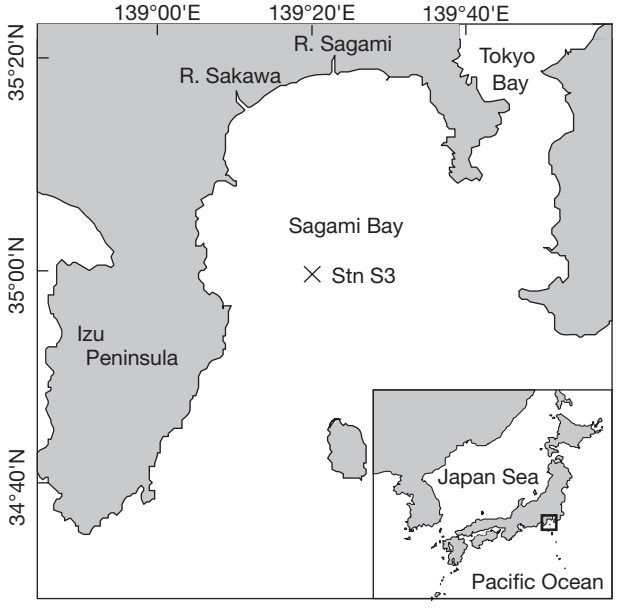

Fig. 5. Location of Stn S3 in the center of Sagami Bay, Japan

($\iint P_{O2}(t,z)\,dz\,dt$) on 18 and 25 April and 9 May, and was compared with previous values recorded at this location by the oxygen evolution method (Hashimoto et al. 2005). From Falkowski (1981), ψ_{O2} was determined as:

$$\Psi_{O2} = \frac{\iint P_{O2}(t,z)\,dz\,dt}{\int \text{chl } a(z)\,dz \times \int E_0(t)\,dt} \quad (2)$$

where $\int E_0(t)dt$ is the surface irradiance (E_0) integrated over 24 h. For integrated chl *a* concentration from the surface to the base of the euphotic layer ($\int$chl $a(z)dz$), we used the mean of 6 measurements from 8:00 to 18:00 h.

RESULTS AND DISCUSSION

Surface seawater temperature increased from 15°C on 15 April 2005 to 18°C on 10 May 2005 (Fig. 6a). The water column was gradually stratified from the end of April. Salinity ranged from 34.2 to 34.6 psu (Fig. 6b). Low salinity of <34.3 psu was recorded in the shallow layers (<20 m) owing to the inflow of coastal waters. Chl *a* concentration increased gradually, and peaks with >5 mg chl *a* m^{-3} were observed (Fig. 6c). During the study period, a time series of chl *a* maps from the Sea-viewing Wide Field-of-view Sensor (SeaWiFS) Project showed that widespread phytoplankton blooms occurred on the eastern coast of Japan, including in the Sagami Bay (K. Sasaoka pers. comm.). The profiling buoy system would have detected part of these widespread phytoplankton blooms. The vertical distribution of chl *a* was closely linked to depth, and a high chl *a* concentration was observed in the upper mixed layer. Development of phytoplankton blooms resulted in a shoaling of the 1% light penetration level (relative to 0 m) from 60 m to 20–30 m, owing to enhanced light attenuation with increasing chl *a* concentration (Fig. 6d).

F_v/F_m is generally used as an index of potential photochemical efficiency. A high F_v/F_m means that the energy transfer between photosystems is well coupled, with low energy loss (as heat and fluorescence), and the light energy absorbed is efficiently utilized in photosynthesis (Falkowski & Raven 1997). The profile of F_v/F_m showed low values at the surface (about 10 m), increasing to >0.5 through the mixed layer below the surface, and then decreasing again below the mixed layer (Fig. 6e). High concentrations of chl *a* were observed in the layer with high F_v/F_m in the water column (Fig. 6c,e). Thus, high F_v/F_m would have promoted the development of phytoplankton blooms. σ_{PSII} is a measure of the efficiency of energy transfer from the antenna pigments to the PSII reaction centers; it represents the amount of light energy usable for

photochemical reactions (Mauzerall & Greenbaum 1989, Kolber et al. 1998). Here, low values of σ_{PSII} (<500 Å^2 quanta^{-1}) were observed in the mixed layer, whereas high values of σ_{PSII} occurred below the mixed layer (Fig. 6f). This change in σ_{PSII} would have been due to adjustment of the absorption capability of individual phytoplankton (a decrease in size of the antenna serving PSII reaction centers and a shift from photosynthetic pigments to nonphotosynthetic pigments) (Falkowski & Raven 1997) and/or a change in the phytoplankton composition of the water column.

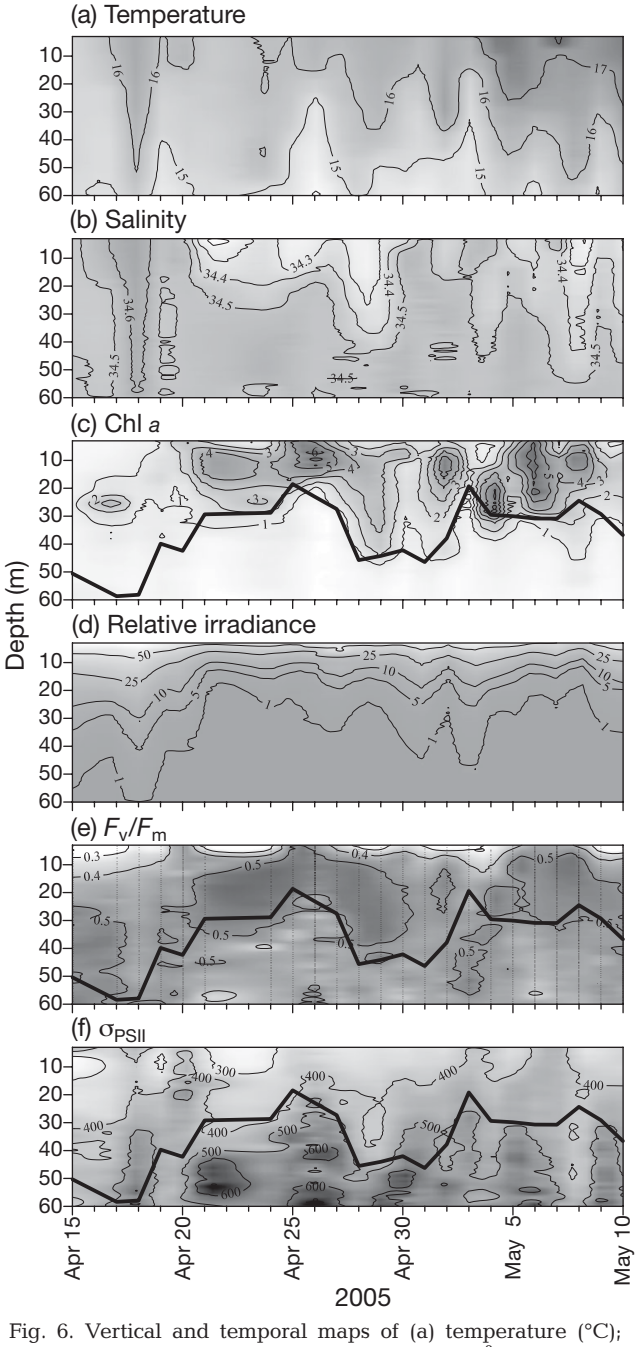

Fig. 6. Vertical and temporal maps of (a) temperature (°C); (b) salinity (psu); (c) chl *a* concentration (mg m^{-3}); (d) relative irradiance (to 0 m); (e) potential photochemical efficiency of open reaction centers (F_v/F_m); and (f) effective absorption cross-section of PSII in darkness (σ_{PSII}), measured at 10:00 h daily during the investigation period. The bold line in (c), (e) and (f) denotes the upper mixed layer, defined as the depth where a steep variation in density (sigma-t) was observed. Vertical dotted lines in (e) represent the FRR measurement points

Integrated chl *a* concentration ($\int$chl $a[z]dz$) and P_{O2} ($\int P_{O2}[z]dz$) from the surface to the base of the euphotic layer are shown in Fig. 7. $\int P_{O2}(z)dz$ increased gradually with $\int$chl $a(z)dz$, and the maximum $\int P_{O2}(z)dz$ of 49.4 mmol O_2 m^{-2} h^{-1} was estimated on 2 May 2005, when both E_0 and $\int$chl $a(z)dz$ were relatively high. $\int$chl $a(z)dz$ and $\int P_{O2}(z)dz$ showed upward trends with time, suggesting that phytoplankton productivity was largely enhanced along with bloom development over the duration of the study. If we assume our observation period covered the initial to the main phases of phytoplankton bloom, then the development of blooms enhanced $\int P_{O2}(z)dz$ in this region by about 5 times. The variations in $\int P_{O2}(z)dz$ were related to the irradiance, the concentration and distribution of chl *a*, and the physiological state of the phytoplankton community. Above all, the variations were dependent on the irradiance and chl *a* concentration.

Several earlier investigations pointed out that the largest uncertainty in using FRR fluorometry to estimate primary productivity is the assumption of n_{PSII} for the conversion of photosynthetic rate per unit PSII reaction center to photosynthetic rate per unit chl *a* (Raateoja & Seppälä 2001, Suggett et al. 2001, Smyth et al. 2004). Because n_{PSII} is not easily measured in natural phytoplankton communities, we used a typical value of n_{PSII} (0.002) for estimating P_{O2} (Kolber & Falkowski 1993). Thus, the assumption of n_{PSII} may have introduced an error in the estimation of P_{O2}. In the present study, it is hard to quantitatively assess the error in the estimation of P_{O2}. Therefore, we attempted to validate $\iint P_{O2}(t,z)dzdt$ indirectly. The $\iint P_{O2}(t,z)dzdt$ on 18 and 25 April and 9 May 2005, as calculated from the data measured at 2 h intervals, was 180, 275, and 311 mmol O_2 m^{-2} d^{-1}, respectively. Using Eq. (2), ψ_{O2} calculated from both FRR fluorometry (the present study) and the oxygen evolution method (Hashimoto et al. 2005) were plotted as a function of $\int E_0(t)dt$ (Fig. 8). The ψ_{O2} derived from FRR fluorometry were in the range of previous independent estimates by the oxygen evolution method, suggesting that our observations by FRR fluorometry were able to roughly estimate the daily P_{O2} *in situ*. This consideration is supported by results of Sarma et al. (2006), who found that the $\iint P_{O2}(t,z)dzdt$ estimated from FRR fluorometry showed good agreement with those estimated by the oxygen isotopes ($^{17}\Delta$ anomaly) method (Luz & Barkan 2000) and ^{18}O spike incubation method (Bender et al. 2000) in this region.

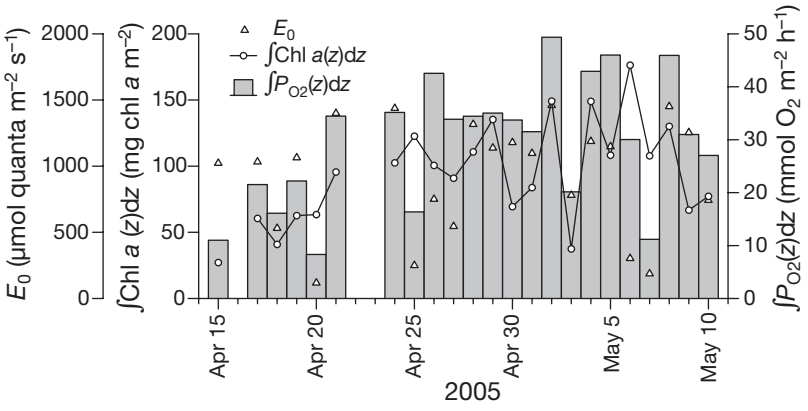

Fig. 7. Temporal variations in surface irradiance (E_0) and chl *a* concentration ($\int$chl *a*(*z*)d*z*) and P_{O2} ($\int P_{O2}(z)dz$) vertically integrated from the surface to the base of the euphotic layer

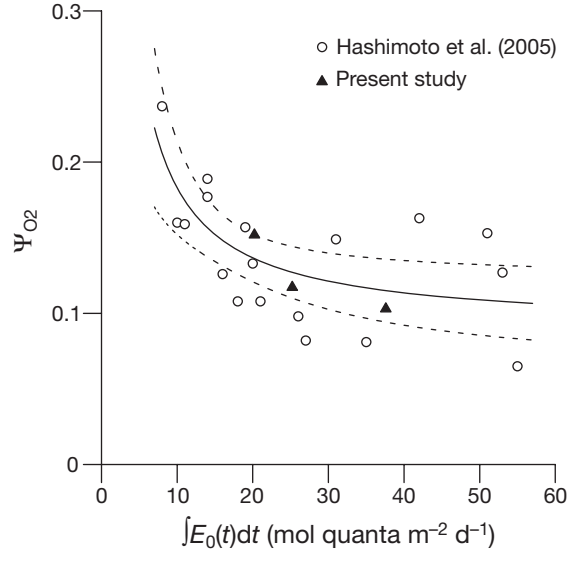

Fig. 8. Light utilization efficiency of a water column (ψ_{O2}) in relation to integrated E_0 over 1 d ($\int E_0(t)dt$), as derived by the oxygen evolution method (Hashimoto et al. 2005) and FRR fluorometry (present study). Values of ψ_{O2} were calculated by Eq. (2). (- - -): 95% CI for the estimations of Hashimoto et al. (2005)

By using the profiling buoy system with the FRR fluorometer, we were able to obtain not only the vertical profiles of PSII parameters and P_{O2} but also the temporal variations in these estimates. It is also important to note that P_{O2} measured by the profiling buoy system had greater vertical and temporal resolutions than measurements based on traditional bottle incubations. This advantage allowed us to detect phytoplankton blooms. The results suggest that the profiling buoy system is a valuable tool for revealing the relationship between phytoplankton productivity and environmental variables of the ocean.

The current understanding of phytoplankton productivity in aquatic ecosystem research is based mostly on estimation per day (Marra 2002). To obtain daily estimates of productivity, we performed measurements with the profiling buoy system at approximately 0.5 m in depth at 2 h intervals from 8:00 to 18:00 h. Diurnal changes in P_{O2} were strongly dependent on chl *a* concentration and ambient irradiance (data not shown). In addition, low irradiance due to cloud cover caused a transient decrease in P_{O2}. Under such highly variable conditions, the accurate estimation of daily productivity in the investigation area would require measurements at higher vertical and temporal resolutions throughout the daytime. However, measuring at higher resolution produces a sharp increase in the system's battery power consumption and thus reduces the length of the observation period. Therefore, to observe long-term daily productivity with the profiling buoy system, more work is required to estimate daily productivity from fewer measurements.

The profiling buoy system has 2 other advantages. First, shadowing by other objects (e.g. ship and platform) of sensors is problematic for optical measurements. In our buoy system, there is no object at the top of the observation buoy, thereby eliminating shadow effects. Second, if the instruments are moored at shallow depth, the risk of collision between the instruments and ships is enhanced. As the observation buoy is placed at 150 m depth, except for the measurement period, the risk of collision can be greatly reduced. On the other hand, there are some concerns about the profiling buoy system. In order to understand the overall biomass and production of aquatic ecosystems, it is important to estimate the rate of carbon fixation rather than oxygen production. Because the FRR fluorometry measures the rate of electron transport in PS II, it is not easy to estimate carbon fixation compared with oxygen production (Suggett et al. 2001). Hence, care should be taken when the FRR-based oxygen production is transformed into carbon fixation by the photosynthetic quotient. Biofouling is also an issue, as it is the primary limiting factor for autonomous platforms used in aquatic observation. Although our buoy system has succeeded in reducing the biofouling of instruments over approximately 1 mo (see 'Materials and Methods'), the effect of long-term mooring (months to years) is not known exactly. For long-term mooring, further improvements of the profiling buoy system may be required.

One goal in aquatic ecosystem research is to gain a better understanding of how phytoplankton productivity is affected by changes in the physical and chemical structure of the upper ocean. As a means of achieving this goal, the profiling buoy system, with its FRR fluorometer, has potential benefits, because this system can measure *in situ* productivity over vertical and temporal resolutions that are unprecedented in aquatic ecosystem research. Application of this profiling buoy system likely will have a great impact on future aquatic ecosystem research.

Acknowledgements. The authors thank M. Y. Gorbunov and P. G. Falkowski for advice in development of the FRR fluorometer; and T. Nakamura and K. Matsumoto for help with design of the profiling buoy system. We also thank V. V. S. S. Sarma, A. Vézina and 3 anonymous reviewers for comments and suggestions on this manuscript. This work was supported by the CREST (Core Research in Evolutional Science and Technology) and the SORST (Solution Oriented Research for Science and Technology) programs of the Japan Science and Technology Agency.

LITERATURE CITED

Behrenfeld MJ, Esaias WE, Turpie KR (2002) Assessment of primary production at the global scale. In: Williams PJleB, Thomas DN, Reynolds CS (eds) Phytoplankton productivity: Carbon assimilation in marine and freshwater ecosystems. Blackwell Science, Oxford, p 156–186

Bender ML, Dickson ML, Orchardo J (2000) Net and gross production in the Ross Sea as determined by incubation experiments and dissolved O_2 studies. Deep-Sea Res II 47: 3141–3158

Corno G, Letelier RM, Abbott MR, Karl DM (2005) Assessing primary production variability in the North Pacific Subtropical Gyre: a comparison of fast repetition rate fluorometry and ^{14}C measurements. J Phycol 42:51–60

Falkowski PG (1981) Light-shade adaptation and assimilation numbers. J Plankton Res 3:203–216

Falkowski PG, Kolber Z (1995) Variations in chlorophyll fluorescence yields in phytoplankton in the world oceans. Aust J Plant Physiol 22:341–355

Falkowski PG, Raven JA (1997) Aquatic photosynthesis. Blackwell Science, Oxford

Fujiki T, Toda T, Kikuchi T, Aono H, Taguchi S (2004) Phosphorus limitation of primary productivity during the spring-summer blooms in Sagami Bay, Japan. Mar Ecol Prog Ser 283:29–38

Hashimoto S, Horimoto N, Yamaguchi Y, Ishimaru T, Saino T (2005) Relationship between net and gross primary production in the Sagami Bay, Japan. Limnol Oceanogr 50: 1830–1835

Kolber Z, Falkowski PG (1993) Use of active fluorescence to estimate phytoplankton photosynthesis in situ. Limnol Oceanogr 38:1646–1665

Kolber ZS, Prášil O, Falkowski PG (1998) Measurements of variable chlorophyll fluorescence using fast repetition rate techniques: defining methodology and experimental protocols. Biochim Biophys Acta 1367:88–106

Laney SR (2003) Assessing the error in photosynthetic properties determined by fast repetition rate fluorometry. Limnol Oceanogr 48:2234–2242

Luz B, Barkan E (2000) Assessment oceanic productivity with the triple-isotope composition of dissolved oxygen. Science 288:2028–2031

Marra J (2002) Approaches to the measurement of plankton production. In: Williams PJLeB, Thomas DN, Reynolds CS (eds) Phytoplankton productivity: carbon assimilation in marine and freshwater ecosystems. Blackwell Science, Oxford, p 78–108

Mauzerall D, Greenbaum NL (1989) The absolute size of a photosynthetic unit. Biochim Biophys Acta 974:119–140

Moore CM, Suggett D, Holligan PM, Sharples J and others (2003) Physical controls on phytoplankton physiology and production at a shelf sea front: a fast repetition-rate fluorometer based field study. Mar Ecol Prog Ser 259: 29–45

Nakata N (1985) Sagami Bay: biology. In: Oceanographic Society, Coastal Oceanography Research Committee (ed) Coastal oceanography of Japanese Islands. Tokai University Press, Tokyo, p 417–427 (in Japanese)

Oxborough K, Baker NR (1997) Resolving chlorophyll *a* fluorescence images of photosynthetic efficiency into photochemical and non-photochemical components: calculation of *qP* and *Fv*′/*Fm*′ without measuring *Fo*′. Photosynth Res 54:135–142

Raateoja MP, Seppälä J (2001) Light utilization and photosynthetic efficiency of *Nannochloris* sp. (Chlorophyceae) approached by spectral absorption characteristics and fast repetition rate fluorometry (FRRF). Boreal Env Res 6: 205–220

Raateoja MP, Seppälä J, Kuosa H (2004) Bio-optical modeling of primary production in the SW Finnish coastal zone, Baltic Sea: fast repetition rate fluorometry in Case 2 waters. Mar Ecol Prog Ser 267:9–26

Sarma VVSS, Abe O, Hinuma A, Saino T (2006) Short-term variation of triple oxygen isotopes and gross oxygen production in the Sagami Bay, central Japan. Limnol Oceanogr 51:1432–1442

Smyth TJ, Pemberton KL, Aiken J, Geider RJ (2004) A methodology to determine primary production and phytoplankton photosynthetic parameters from fast repetition rate fluorometry. J Plankton Res 26:1337–1350

Steemann Nielsen E (1952) The use of radioactive carbon (^{14}C) for measuring organic production in the sea. J Cons Intl Expl Mer 18:117–140

Suggett D, Kraay G, Holligan P, Davey M, Aiken J, Geider R (2001) Assessment of photosynthesis in a spring cyanobacterial bloom by use of a fast repetition rate fluorometer. Limnol Oceanogr 46:802–810

Suggett DJ, Moore CM, Oxborough K, Geider RJ (2006) Fast repetition rate (FRR) chlorophyll *a* fluorescence induction measurements. Chelsea Technologies Group, West Molesey, p 1–53, available at www.chelsea.co.uk/Technical%20Papers/FRRFmethodsManual.pdf

Williams PJLeB, Heinemann KR, Marra J, Purdie DA (1983) Comparison of ^{14}C and O_2 measurements of phytoplankton production in oligotrophic waters. Nature 305:49–50

Editorial responsibility: Alain Vézina (Contributing Editor), Dartmouth, Nova Scotia, Canada

Submitted: January 12, 2007; Accepted: July 10, 2007
Proofs received from author(s): December 26, 2007